Extended Electronic Interactions in a Triangular μ-Oxotriruthenium Acetate Cluster Containing Nitric Oxide

Henrique E. Toma,*[a] Anamaria D. P. Alexiou,[a] and Sergio Dovidauskas[a]

Keywords: Ruthenium / Nitrogen oxides / Carboxylate ligands / Cluster compounds / Pi interactions

The binding of NO to the trinuclear cluster $[Ru_3O(CH_3CO_2)_6(py)_2]^+$ (py = pyridine) leads to a stable, diamagnetic $[Ru_3O(CH_3CO_2)_6(py)_2(NO)]^+$ complex, displaying extended electronic interactions which arise from the coupling of the unpaired π^* electron of NO and the unpaired electron in the π-orbitals of the Ru_3O unit. This complex has been isolated and its spectroscopic characterization (EPR, ^1H and ^{13}C NMR, IR, UV/Vis) and electrochemical/spectroelectrochemical properties are reported in this paper. The NO^0 character in the complex is supported by spectroscopic and electrochemical results, as well as by semi-empirical theoretical calculations carried out for the complex. A remarkable point in this system is the dramatic changes in the Ru–NO electronic interactions accompanying the several successive redox states of the triangular Ru_3O center.

Introduction

Triangular μ-oxoruthenium acetate clusters of general formula $[Ru_3O(CH_3CO_2)_6L_3]^n$ (L = H_2O, N-heterocycles, etc.) are particularly interesting because of their rich mixed-valence chemistry, displaying catalytic properties and versatility as building blocks in supramolecular chemistry.[1] This type of complex exhibits a series of successive oxidation states and the corresponding redox potentials are dependent of the pK_a [2] and E_L parameters[3] of the terminal ligands. In general, clusters containing all ruthenium ions in the formal oxidation state +3 and above are preferentially stabilized by σ-donor ligands (L). Mixed-valence clusters with the formal oxidation state $Ru^{III}Ru^{III}Ru^{II}$, and below, are stabilized by π-acceptor molecules such as CO[4–6] or isocyanide ligands.[7,8]

Nitric oxide is a typical non-innocent ligand. It can bind to a metal center (M) yielding a metal-nitrosyl complex, where the ligand can be classified as NO^+, $NO^{\cdot}$ or NO^-.[9–12] In recent years a great number of reports dealing with NO activity in biological systems have been published,[13–20] and ruthenium nitrosyl complexes have been exploited as potential scavengers or delivery drugs for NO into biological targets.[21–27]

Because of the several available oxidation states, the interaction between NO and the triangular μ-oxoruthenium acetate clusters can be viewed as a puzzling question, especially concerning the electronic delocalization and the nature of the redox orbitals involved. Such important aspects have been focused on in this work, starting from the synthesis and characterization of the novel clusters species $[Ru_3O(CH_3CO_2)_6(py)_2(NO)]PF_6$ (Figure 1), and carrying out a detailed investigation of its spectroscopic and electrochemical properties, and a theoretical simulation of its electronic structure based on semi-empirical methods. To the best of our knowledge, except for a brief comment by Spencer and Wilkinson on the interaction of nitric oxide with $[Ru_3O(CH_3CO_2)_6L_3]^+$ [L = CH_3OH and $P(C_6H_5)_3$] complexes,[4] the chemistry of this type of nitrosyl-triruthenium acetate cluster has never been reported before.

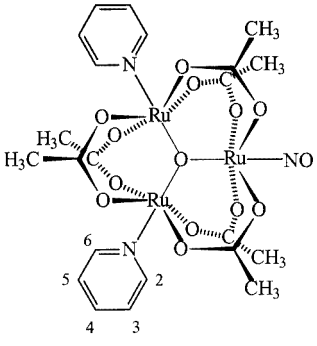

Figure 1. Structural representation of $[Ru_3O(CH_3CO_2)_6(py)_2(NO)]PF_6$; the labels of pyridine hydrogen atoms are required for the analysis of the NMR spectra

Results and Discussion

The general route for the synthesis of Ru–NO complexes based on the procedures involving $NaNO_2$ and acids[28] was initially attempted in this work, but resulted in low yields

[a] Instituto de Química, Universidade de São Paulo,
C. Postal 26077, CEP05513–970, Brazil
Fax: (internat.) +55-11/3815-5579
E-mail: henetoma@iq.usp.br

Supporting information for this article is available on the WWW under http://www.eurjic.org or from the author.

and an impure product. Surprisingly, the direct reaction of $[Ru_3O(CH_3CO_2)_6(py)_2(CH_3OH)]^+$ and NO was successful, yielding a rather stable complex, isolated as $[Ru_3O(CH_3CO_2)_6(py)_2(NO)]PF_6 \cdot CH_2Cl_2$. Its thermal stability was assayed by thermogravimetry, showing solvent loss in the range 100−253 °C and decomposition of the cluster above this temperature, indicating that the Ru−NO bonding is quite strong.

The first question concerning the nature of the $[Ru_3O(CH_3CO_2)_6(py)_2(NO)]^+$ complex refers to its valence description, for example, as $Ru^{III}Ru^{III}Ru^{III}NO^0$ or $Ru^{III}Ru^{III}Ru^{II}NO^+$, in a formal representation. For discussion purposes, the starting $[Ru_3O(CH_3CO_2)_6(py)_2(CH_3OH)]^+$ was taken as a reference compound exhibiting a formal $Ru^{III}Ru^{III}Ru^{III}$ oxidation state. In the other extreme, the $[Ru_3O(CH_3CO_2)_6(py)_2(CO)]$ complex provides a suitable model illustrating the effects of the strong π-acceptor CO ligand in preferentially stabilizing the formal $Ru^{III}Ru^{III}Ru^{II}(CO)$ oxidation state. NO^+ is a stronger π-acceptor ligand than CO, therefore if the $[Ru_3O(CH_3CO_2)_6(py)_2(NO)]^+$ complex involves NO^+, its acceptor properties would exceed those of the CO analog in terms of π-backbonding effects. In contrast, in the NO^0 form the available π*-electron can preferentially stabilize the $Ru^{III}Ru^{III}Ru^{III}$ cluster by coupling with the ruthenium d_π-electrons. In fact, such an electronic balance is supposed to be very delicate, and the NO^+ or NO^0 character will actually depend upon the relative energies of the metal cluster and NO frontier orbitals.

The complex $[Ru_3O(CH_3CO_2)_6(py)_2(NO)]PF_6 \cdot CH_2Cl_2$ exhibits a small room temperature molar paramagnetic susceptibility (6.7×10^{-4} cgs unit) very similar to that determined under the same conditions for the complex $[Ru_3O(CH_3CO_2)_6(py)_2(CO)] \cdot C_6H_6$ (6.8×10^{-4} cgs unit). Presumably, the small paramagnetism in both complexes reflects the temperature-independent paramagnetic susceptibility arising from the mixing with the excited states, which has previously been estimated to fall within the range $2.3-27 \times 10^{-4}$ cgs unit.[29,30] No EPR signal was seen at either room or liquid nitrogen temperatures for the complex $[Ru_3O(CH_3CO_2)_6(py)_2(NO)]PF_6$, thus suggesting a strong coupling between the available π*-electron in NO^0 and the ruthenium d_π-electrons in the $Ru^{III}Ru^{III}Ru^{III}$ cluster.

Infrared Spectra

The FTIR spectrum of the cluster $[Ru_3O(CH_3CO_2)_6(py)_2(NO)]PF_6$ (Figure 2) was assigned by comparison with the data for $[Ru_3O(CH_3CO_2)_6(py)_2(CH_3OH)]PF_6$ and similar compounds described in the literature[5,31−33] (FTIR data and assignments are available as Supporting Information). The characteristic peak for the nitrosyl group is found at 1865 cm^{-1} (Figure 2), corresponding to the ν(NO) vibration. This peak is very strong and symmetric, and is not observed in the spectrum of the complex $[Ru_3O(CH_3CO_2)_6(py)_2(CH_3OH)]PF_6$. Another important observation supporting the strong binding of NO is that practically all vibrational modes of the coordinated ligands are changed in the NO complex as a consequence of the electronic perturbation. For instance, the $\nu_{as}(COO^-)$ vibrational peak observed at 1550 cm^{-1} for the methanol complex, is shifted to 1585 cm^{-1} in the NO compound.

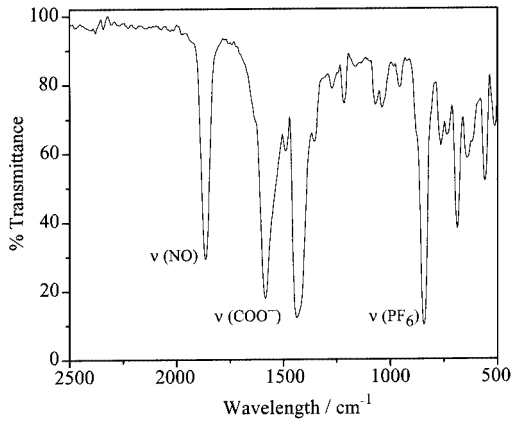

Figure 2. FT-IR spectrum of the $[Ru_3O(CH_3CO_2)_6(py)_2(NO)]PF_6$ cluster

It should be noted that the ν(NO) peak of free NO is located at 1876 cm^{-1}, but in the metal complexes it is very sensitive to the binding properties and oxidation states of the metal ion. For instance, ν(NO) frequencies for *cis*-$[Ru^{II}(bipy)_2(NO)L]$ complexes (L = N^{3-}, Cl^-, NO_2^-, NH_3, py, CH_3CN) have been observed in the range 1923−1970 cm^{-1}.[34] For $[Ru^{II}(NH_3)_5(NO)]^{3+}$ [35] and *trans*-$[Ru^{II}(NH_3)_4(NO)L]$[36] complexes [L = imidazole, L-histidine, py, isonicotinamide, pyrazine, $P(OEt)_3$], ν(NO) values span the range 1909−1941 cm^{-1}, whereas for L = SO_3^{2-}, ν(NO) = 1871 cm^{-1}. In the case of *trans*-$[Ru^{II}(py)_4(NO)L]$[37] complexes, for L = Cl^-, and Br^-, ν(NO) = 1910 and 1901 cm^{-1}, respectively, but for L = OH^-, ν(NO) = 1860 cm^{-1}. In all such examples, the ruthenium center has been considered as mainly Ru^{II}, thus imputing a predominantly NO^+ character to the nitrosyl ligand. In the case of the reduced complexes $[Ru(bipy)_2(NO)(CH_3CN)]^{2+}$ and $[Ru(bipy)_2(NO)Cl]^+$ ν(NO) is shifted to 1665 and 1640 cm^{-1}, and the spectroscopic and electrochemical data support the hypothesis of NO^+ reduction, yielding NO^0 species.[34]

In the case of *trans*-[Ru(dimethylglyoximato)(NO)Cl],[38] ν(NO) = 1878 cm^{-1} and is very close to the frequency of the free nitric oxide molecule, although a significant NO^+ character has been suggested from its observed reactivity in the presence of nucleophiles.[39] Perhaps because of its partial NO^0 character, only a small shift of ν(NO) to 1855 cm^{-1} is observed in this system upon reduction.

In the complex $[Ru_3O(CH_3CO_2)_6(py)_2(NO)]^+$, the observed ν(NO) frequency (1865 cm^{-1}) falls in the range characteristic of linear nitrosyl complexes M−NO,[12] and is closer to the vibrational frequency of free NO (1876 cm^{-1}) than of NO^+ (2273 cm^{-1}) or NO^- (1358−1374 cm^{-1}). However, it should be noted that in the NO^+ complexes the ν(NO) frequencies can also decrease significantly as a consequence of π-backbonding interactions, and typical values have been observed in the range of 1900−1970 cm^{-1} as shown by the preceding examples. In special cases (as in

the nitrosyl cluster system herein reported) where ν(NO) is close to that of the free NO molecule, the differentiation between a typical NO^0 complex and the case involving a rather strong π-backbonding to NO^+ is not obvious and cannot be carried out exclusively on the basis of the infrared vibrational data.

^{1}H and ^{13}C NMR Spectra

The ^{1}H and ^{13}C NMR spectra of the cluster were assigned by comparison with related clusters[1,5−7,40−52], using peak integration and COSY (^{1}H,^{1}H) and HMQC (^{1}H, ^{13}C) bidimensional techniques (see also Supporting Information). In the ^{1}H and ^{13}C NMR spectra one can observe two signals for the CH_3 groups, in accordance with the C_{2v} cluster symmetry. Selected NMR spectroscopic data are collected in Table 1 in order to illustrate how the signals of the ligands coordinated to the Ru_3O core depend upon the oxidation states of the ruthenium ions. Reduced clusters in the $Ru^{III}Ru^{III}Ru^{II}$ formal oxidation state, including CO species, are diamagnetic and show coordinated ligand signals close to the free ones and slightly downfield shifted. On the other hand, the oxidized clusters ($Ru^{III}Ru^{III}Ru^{III}$) are paramagnetic and their signals are not only sensitive to the inductive effects from the metal center, but also to the paramagnetic anisotropy of the Ru_3O unit.[47] Interestingly, the CH_3 and H_2 proton signals of acetate and pyridine are found at chemical shifts between the signals of the diamagnetic $[Ru_3O(CH_3CO_2)_6(py)_2CO]^0$, $[Ru_3O(CH_3CO_2)_6(py)_3]^0$ and the paramagnetic $[Ru_3O(CH_3CO_2)_6(py)_3]^+$ clusters. This rules out a description in terms of a formal $Ru^{III}Ru^{III}Ru^{II}NO^+$ oxidation state, since its corresponding NMR spectra would be similar to the CO analog.

The NMR spectroscopic data suggest a significant NO^0 character in the cluster system. The formal representation $Ru^{III}Ru^{III}Ru^{III}NO^0$ should be interpreted rather carefully, since there is a strong coupling between the NO^0 π*-electron and the ruthenium d_π-electrons, which results in a large diamagnetism according to magnetic susceptibility measurements. In fact, the increase in the π-electron density is reflected in the *J* values observed for the pyridine ligand signals [$^3J_{H,H}$ = 6.5 Hz, C(2)−H; $^4J_{H,H}$ = 1.5 Hz, C(2)−H; $^3J_{H,H}$ = 7.6 Hz, C(3)−H]. In the oxidized clusters these constants are too small to be observed because the scalar coupling decreases as the oxidation state of the coupled nucleus increases.[53] The CH_2Cl_2 molecule was detected in the ^{1}H and ^{13}C NMR spectra at δ = 5.32 and 55 ppm, respectively, corroborating the elemental analysis and thermogravimetry results.

Electronic Structure

The electronic spectrum of $[Ru_3O(CH_3CO_2)_6(py)_2(NO)]PF_6$ exhibits a series of superimposed bands in the 300−800 nm range, which can be deconvoluted as shown in Figure 3. The absorption profile is rather unusual, displaying apparently little similarity with those reported in the literature for related complexes.[2,6,7]

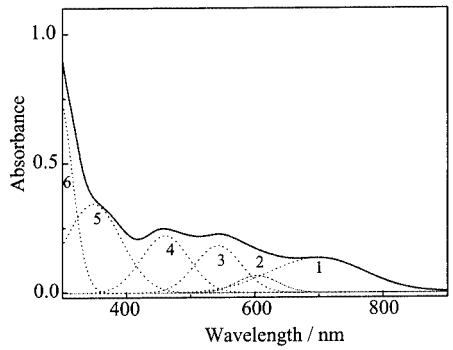

Figure 3. Electronic spectrum of a 10^{-3} M $[Ru_3O(CH_3CO_2)_6(py)_2(NO)]PF_6$ solution in acetonitrile

The electronic structure of $[Ru_3O(CH_3CO_2)_6L_3]$ clusters has been discussed in terms of a qualitative molecular orbital scheme proposed by Cotton and Norman, centered on the Ru_3O π-system in D_{3h} symmetry.[54] In this scheme, the central oxygen atom is considered to be sp^2 hybridized, leaving a single p_z orbital of π symmetry to interact with the ruthenium d_π orbitals ($d_{zy'}$, $d_{x'z}$, and $d_{x'^2-y'^2}$). The Ru $d_{zy'}$ orbitals are perpendicular to the horizontal symmetry plane of the molecule, and can combine with the O p_z orbital,

Table 1. ^{1}H and ^{13} C NMR chemical shifts (δ) for the $[Ru_3O(CH_3CO_2)_6L_3]^n$ (Ru_3L_3) clusters in CD_3CN

	$Ru_3^{III,III,III}py_3$ [47]	$Ru_3^{III,III,III}py_2NO$	$Ru_3^{III,III,II}py_2CO$[40]	$Ru_3^{III,III,II}py_3$ [a] [5]
			^{1}H (ppm)	
H_3C	4.82 (12 H)	3.96 (12 H)	2.10 (6 H)	2.14 (17.8 H)
		3.28 (6 H)	2.16[b]	
$H_{2,6}$ (L)	0.25 (6 H)	4.49 (4 H)	9.14 (4 H)	9.02 (6.0 H)
$H_{3,5}$ (L)	5.82 (6 H)	8.18 (4 H)	8.13 (4 H)	7.69 (6.1 H)
H_4 (L)	6.57 (3 H)	5.82 (2 H)	8.31 (2 H)	7.99 (3.2 H)
			^{13}C (ppm)	
H_3C	−6.4	9.1	30.8	
		16.4		
COO^-	199.3	221.2	212.5	
$C_{2,6}$ (L)	126.6	162.1	154.4	
$C_{3,5}$ (L)	114.5	113.7	126.5	
C_4 (L)	138.1	152.4	142.6	

[a] In CD_2Cl_2. [b] Overlapped with water signal.

giving rise to two a_2'' molecular orbitals, while the $d_{zy'} - d_{zy'}$ combination leads to an e'' molecular orbital. The Ru $d_{x'z}$ orbitals are localized in the Ru_3O plane and their direct combination gives rise to e'(1) and a_2' molecular orbitals. The remaining Ru $d_{x'^2-y'^2}$ orbitals can interact weakly since a considerable distance separates them. However, these orbitals can interact with the p orbitals localized on the oxygen atoms of the bridging acetates, providing a further mechanism for Ru−Ru interactions. This would remove the degeneracy of the three $d_{x'^2-y'^2}$ orbitals, giving rise to e'(2) and a_1' levels.

Under C_{2v} symmetry, the a_2'', a_2', and a_1' levels transform according to b_1, b_2, and a_1, while the e'' and e' levels split into b_1, a_2, and a_1, b_2, respectively. In principle, the qualitative molecular orbital diagram proposed by Cotton and Norman could be employed for extrapolating to C_{2v} symmetry based on a simple correlation procedure. In our case, however, this is not feasible, since the π-interactions with the NO ligand make the qualitative ordering of the molecular orbitals rather complicated.

In order to shed some light on the electronic structure of the nitrosyl cluster, a preliminary molecular orbital calculation was carried out for the model complex $[Ru_3O(CH_3CO_2)_6(NH_3)_2(NO)]^+$ using the ZINDO/S semi-empirical method after a suitable geometry optimization based on the MM^+ force field, as described in the Exp. Sect. The pyridine ligands were replaced by NH_3 in order to simplify the calculations and, specially, to facilitate the interpretation of the electronic properties of the Ru_3O-NO chromophore. It should be noticed that pyridine and NH_3 are very close in the spectrochemical series of ligands, and their influence in the $Ru^{III}Ru^{III}Ru^{III}$ cluster is expected to be rather similar.

The atomic charge distribution for the model complex can be seen in Figure 4. In this complex, the NO ligand bears a very small negative charge (δ = −0.068) while the attached ruthenium ion has a positive charge (δ = 0.593) that is significantly higher than the other two ruthenium ions (δ = 0.353). Therefore, the charge distribution within the Ru_3O-NO moiety indicates a predominant NO^0 character, and also the occurrence of substantial π-backbonding effects involving the Ru−NO bond.

According to the ZINDO/S molecular orbital calculations (Table 2) the NO ligand has a strong influence on several energy levels, particularly those involving the Ru $d_{zy'}$ (MO 99, 96, 90) and Ru $d_{x'z}$ (MO 100, 98, 91) orbitals. For instance, in the case of MO 100 (LUMO 2) the NO character is 83%, while for MO 99 (LUMO 1) there is a nearly equivalent mixture with the Ru d_π orbitals. Among the HOMO levels, MO 96 and 91 exhibit a high contribution of NO (16%), although the highest contribution is observed for MO 90 (42%).

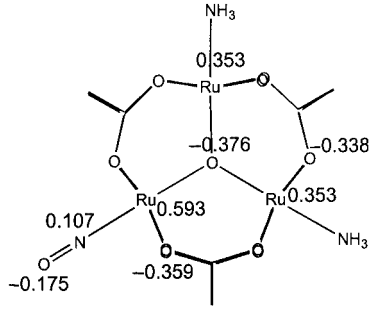

Figure 4. Atomic charge distribution for the model cluster $[Ru_3O(CH_3CO_2)_6(NH_3)_2(NO)]^+$

Table 2. Molecular orbital composition for the cluster $[Ru_3O(CH_3CO_2)_6(NH_3)_2NO]^+$

MO	% Ru	% NO	% CH_3CO_2	% O
		HOMO		
90	42	42	14	
91	63	15	13	6
92	77		22	
93	78		18	2
94	75		18	5
95	82		13	2
96	56	16	10	16
97	65		34	
		LUMO		
98	66	6	27	
99	49	34	6	9
100	14	83	2	

The ZINDO/S method successfully reproduces the observed electronic transitions in the nitrosyl cluster, as shown in Figure 3. Such transitions are also indicated in the molecular orbital scheme (Figure 5) corresponding to symmetry- and spin-allowed transitions. Transition 1, at 691 nm (ε = 1740 $M^{-1}cm^{-1}$), corresponds to the HOMO 0 → LUMO 0 excitation, involving essentially the occupied trinuclear ruthenium-acetate level of a_1 symmetry (MO 97) and the next empty b_2 level (MO 98) displaying some NO character (6%). Transition 2, at 602 nm, is relatively weak, and involves the excitation from MO 97 to MO 99 (b_1), displaying strong NO character. Transition 3, at 538 nm (ε = 2840 $M^{-1}cm^{-1}$), is more intense and involves the excitation from MO 96 (b_1) to MO 99 (b_1); both exhibiting significant NO character. Transition 4, at 451 nm (ε = 3130 $M^{-1}cm^{-1}$), corresponds to excitation from the $Ru_3O(CH_3CO_2)_6$ level [MO 93 (b_2) to MO 98], while transition 5 at 338 nm (ε = 4700 $M^{-1}cm^{-1}$) corresponds, similarly, to the excitation from MO 92 (a_1) to MO 99. The strongest band should correspond to the transition from MO 91 (b_2) to MO 100 (b_2). Unfortunately, in the pyridine complex this band is masked by the strong cluster-to-pyridine charge-transfer bands and also by the internal transitions in the aromatic ligand.

Electrochemical Behavior

The cyclic voltammogram of $[Ru_3O(CH_3CO_2)_6(py)_2(NO)]^+$ is shown in Figure 6 along with those for the reference complexes $[Ru_3O(CH_3CO_2)_6(py)_2(CH_3OH)]^+$ and $[Ru_3O(CH_3CO_2)_6(py)_2(CO)]^0$. The nitrosyl cluster exhibits four successive redox waves at −1.15, −0.44, 1.00 and 1.77 V (vs. Ag/Ag^+), which, in principle, can be ascribed to the

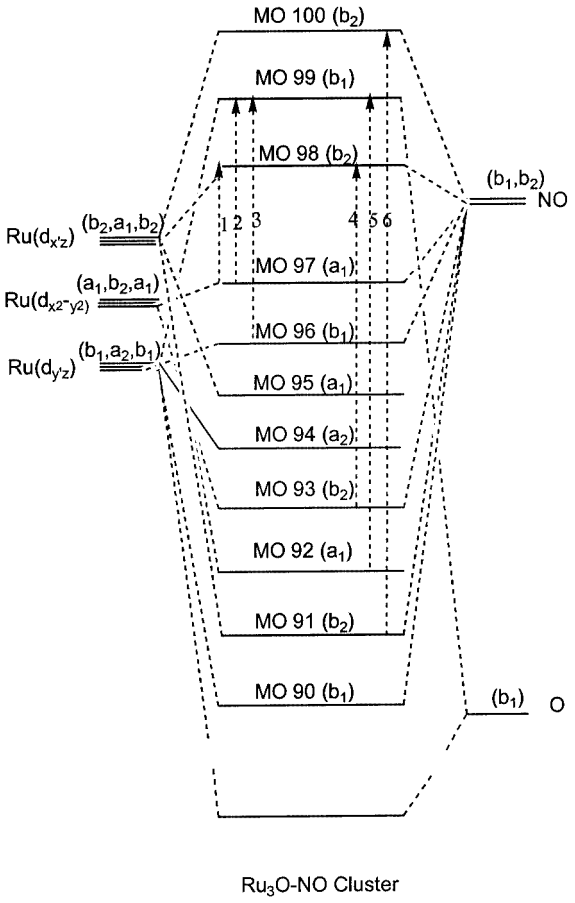

Figure 5. Molecular orbital scheme for the cluster $[Ru_3O(CH_3CO_2)_6(py)_2(NO)]^+$

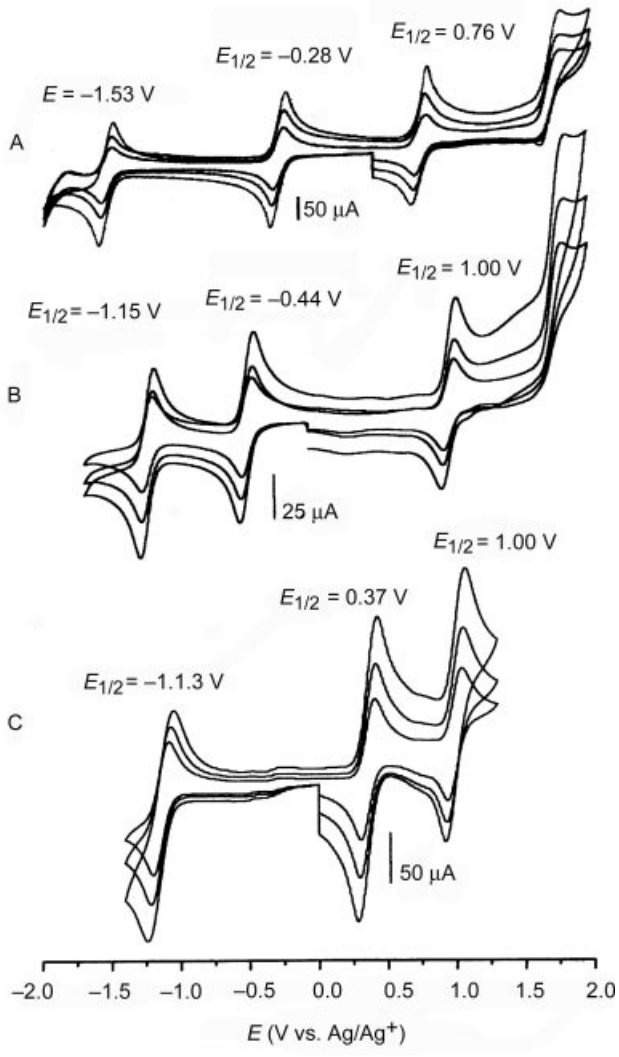

Figure 6. Cyclic voltammogram of the cluster (10^{-3} M), in acetonitrile solution containing 0.1 M $TEAClO_4$: (a) $[Ru_3O(CH_3CO_2)_6(py)_2(CH_3OH)]PF_6$; (b) $[Ru_3O(CH_3CO_2)_6(py)_2(NO)]PF_6$; (c) $[Ru_3O(CH_3CO_2)_6(py)_2(CO)]$

redox couples $Ru^{III}Ru^{II}Ru^{II}/Ru^{III}Ru^{III}Ru^{II}/Ru^{III}Ru^{III}Ru^{III}/Ru^{IV}Ru^{III}Ru^{III}/Ru^{IV}Ru^{IV}Ru^{III}$ by comparison with the reference compounds.

In our previous work we have shown that the redox potentials of $[Ru_3O(CH_3CO_2)_6L_3]$ clusters are correlated with the donor-acceptor properties of L, forming a well-behaved sequence, when the voltammograms are superimposed according to this trend. This type of behavior, however, is not apparent in Figure 6. On the other hand, the assignment of the wave at −0.44V to the NO^+/NO^0 couple cannot be totally discarded, since this process is usually observed in the range −0.6 to +0.3V vs. Ag/Ag^+ [55,56] for typical NO^+ complexes. This kind of ambiguity probably arises from the fact that the interactions of the NO ligand with the Ru d_π orbitals make the canonical structures $Ru^{III}-NO^0 \rightleftarrows Ru^{II}-NO^+$ practically equivalent, since the strong back-bonding interactions involving $Ru^{II}-NO^+$ would also lead to an electronic configuration rather close to $Ru^{III}-NO^0$. As a consequence, the NO ligand can stabilize both the $Ru^{III}Ru^{III}Ru^{III}$ (by acting as NO^0) and the $Ru^{III}Ru^{III}Ru^{II}$ (by acting as NO^+) formal oxidation states, increasing the separation between the corresponding redox waves at −0.44 and 1.00 V (ΔE = 1.44 V) in comparison with the CH_3OH (ΔE = 1.04 V) and CO (ΔE = 0.63 V) reference compounds. This exceptional ability to stabilize both oxidation states is actually responsible for the non-innocent character of the NO ligand in many transition metal complexes.

Visible-UV and IR Spectroelectrochemistry

In contrast to the electrochemical measurements, the spectroelectrochemical results were severely limited by decomposition reactions taking place over the time scale of the experiments (about ten minutes). The only completely reversible spectroelectrochemical behavior was observed at E^0 = −0.44V, corresponding to the $(Ru^{III}Ru^{III}Ru^{III}-NO^0 \rightleftarrows Ru^{III}Ru^{III}Ru^{II}-NO^+)/Ru^{III}Ru^{III}Ru^{II-}NO^0$ redox process. As shown in Figure 7a, the reduction of the $Ru^{III}Ru^{III}Ru^{III}-NO^0$ complex gives rise to a broad band in the visible-near infrared region (λ_{max} = 710 nm) consistent with intermetallic transitions within the $Ru^{III}Ru^{III}Ru^{II}-NO^0$ chromophore,[7,42,57] and to a strong band at 400 nm, characteristic of ruthenium-to-pyridine

charge-transfer transitions involving the $Ru^{III}Ru^{III}Ru^{III}$-pyridine moiety.

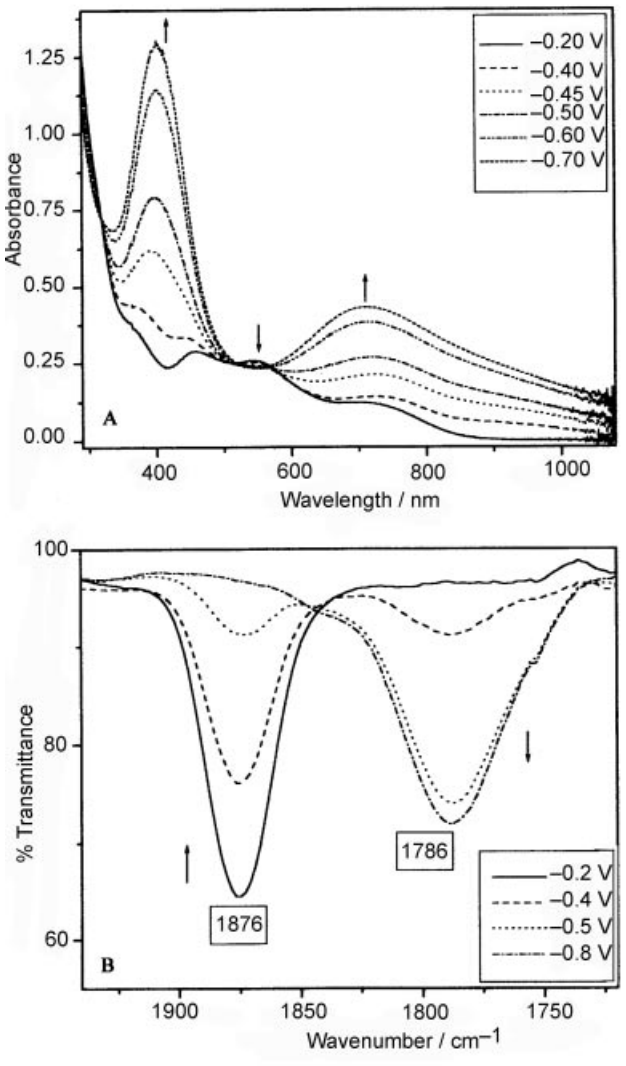

Figure 7. UV/Vis (a) and IR (b) spectroelectrochemistry of $[Ru_3O(CH_3CO_2)_6(py)_2(NO)]PF_6$ (10^{-3} M), in acetonitrile solution containing 0.10 M $TEAClO_4$

The corresponding FTIR spectroelectrochemistry (Figure 7b) exhibits a systematic conversion of the ν(NO) band at 1876 cm^{-1} into a new band at 1786 cm^{-1} indicating some NO^- character, arising from the ($Ru^{II}-NO^0$) back-bonding interactions within the $Ru^{III}Ru^{III}Ru^{II}-NO^0$ chromophore. Above 1.2V and below −1.2V the irreversible decomposition of the nitrosyl-cluster is observed, with the disappearance of the characteristic ν(NO) bands in the FTIR spectrum.

Conclusion

The interaction of NO with the complex $[Ru_3O(CH_3CO_2)_6(py)_2(CH_3OH)]^+$ leads to a stable nitrosyl-cluster system which can be formally described in terms of the delocalized electronic configuration, $Ru^{III}Ru^{III}Ru^{III}-NO^0 \rightleftarrows Ru^{III}Ru^{III}Ru^{II}-NO^+$. The strong involvement of the NO π*-orbitals is supported by theoretical calculations, as well as by the electronic, spectroscopic and magnetic properties of the complex. The remarkable contribution of NO to the LUMO levels accounts for the unusual absorption profiles observed in the electronic spectra of the cluster, as well as a significant photochemical sensitivity: the cluster releases nitric oxide upon irradiation with visible light. This interesting property is currently being investigated in our laboratory, as well as the related biological effects, including the valuation of $[Ru_3O(CH_3CO_2)_6(py)_2(NO)]PF_6$ toxicity.

Experimental Section

General: Tetraethylammonium perchlorate ($TEAClO_4$)[58] and the starting complex $[Ru_3(CH_3CO_2)_6(py)_2(CH_3OH)]PF_6$ were prepared as previously described in the literature.[5] Acetonitrile (HPLC grade, Aldrich) was kept in the presence of 3 Å dry molecular sieves. Other reagents and solvents of analytical grade were used without further purification. Thermogravimetric measurements were performed using a Shimadzu model TGA-50 instrument under the following experimental conditions: 2−4 mg of sample, platinum crucible, N_2 flow of 50 mL·min^{-1}, heating rate of 10 °C·min^{-1}. Infrared spectra were recorded in the region 4000−350 cm^{-1} on a Shimadzu FTIR model 8300 spectrophotometer. The magnetic susceptibilities of powdered samples were measured at room temperature using a Cahn model 7500 electrobalance. The studies in solution were carried out using a 10^{-3} M cluster solution in acetonitrile. X-band EPR spectrum, at 77 K, were conducted with a Bruker EMX spectrometer, operating at 9.53 GHz, 20 MW power and 4−12 G modulation amplitude. ^1H and ^{13}C NMR spectra and two-dimensional COSY (^1H, ^1H) and HMQC (^1H, ^{13}C) spectra were recorded on a Varian INOVA 1 300 MHz and Bruker DRX 500 spectrometers, using a 10^{-2} M cluster solution in CD_3CN. The electronic spectra were recorded on a Hewlett−Packard model 8453 diode-array spectrophotometer, using a 295 nm UV cut-off filter. Cyclic voltammetry and spectroelectrochemistry were carried out with an EG&G model 283 galvanostat/potentiostat. A conventional three-electrode electrochemical cell was used, with a platinum disk as working electrode, a Luggin capillary arrangement with an $Ag/AgNO_3$ (0.01 M) reference electrode in 0.10 M $TEAClO_4$ in acetonitrile, and a platinum wire as auxiliary electrode. UV/Vis spectrochemistry was conducted using a rectangular quartz cell of 0.025 cm internal optical path length, containing an optically transparent gold minigrid electrode, a platinum wire and a small $Ag/AgNO_3$ electrode as working, auxiliary and reference electrodes, respectively. IR spectroelectrochemical measurements were carried out using an acetonitrile solution containing 0.10 M $LiClO_4$ and a homemade IRTRAN thin layer cell, as previously described.[38]

Molecular mechanics geometry optimizations for the model complex $[Ru_3O(CH_3CO_2)_6(NH_3)_2(NO)]^+$ were carried out using the MM^+ module of Hyperchem 6.1 from Hypercube, starting with bond-dipole calculations and stopping at a refinement level of 10^{-3} kcal·$Å^{-1}$·mol^{-1}. In all the attempts, even when using a restricted geometry, the optimization procedure led to a pyramidal Ru_3O structure, rather than to the planar geometry characteristic of this type of system. In order to preserve the planar geometry, the cent-

ral oxygen atom was initially replaced by fluorine, thus allowing a preliminary structural refinement. In the next step, fluorine was replaced by oxygen, and the geometry refinement was carried out again, but stopping just at the point preceding the pyramidal distortion (about 30 cycles). Using this procedure, the central Ru−Ru and Ru−O distances can be adjusted, keeping the oxygen atom inside the triangular ring, without perturbing the remaining, optimized parts of the system. For this frozen undistorted geometry, single-point semi-empirical molecular orbital calculations were carried out, using the spectroscopic implementation of the ZINDO/1 method within the Hyperchem 6.1 package. The semi-empirical method provided the approximate atomic charges, which were used for a new cycle of geometry optimization (MM^+), now replacing the starting bond dipoles. This alternating semi-empirical/molecular mechanics procedure was repeated at least three times, practically ensuring convergence. In this way, the final geometry was planar, exhibiting Ru−Ru(NO) and Ru−Ru distances of 3.257 and 3.266 Å, and three similar Ru−O distances of 1.883 Å; all of them quite similar to the typical crystallographic distances reported in the literature for similar ruthenium acetate clusters.[6,59−61] The theoretical Ru−NO and NO bond lengths were 1.914 and 1.086 Å, respectively. After geometry optimization, the electronic spectra were generated by single CI excitations in an active space involving at least 12 frontier molecular orbitals (seven highest occupied and five lowest unoccupied MOs).

$[Ru_3O(CH_3CO_2)_6(py)_2(NO)]PF_6$: A solution of $[Ru_3(CH_3CO_2)_6(py)_2(CH_3OH)]PF_6$ (0.21 g; 0.21 mmol) in dichloromethane (20 mL) were saturated with Ar for 20 min, then with NO for 15 min (after which the blue solution became violet), and finally with Ar for 20 min. The product was precipitated by adding petroleum ether. The solid was collected on a filter, washed with petroleum ether and dried under vacuum. Yield: 42%. $C_{23}H_{30}Cl_2F_6N_3O_{14}PRu_3$ (1091.6): calcd. C 25.3, H 2.77, N 3.85; found C 25.2, H 2.75, N 3.80. The purity of the final product was confirmed by means of NMR spectroscopy.

Acknowledgments

We are grateful to FAPESP and CNPq for financial support, and to Prof. Ana Maria da Costa Ferreira for conducting the EPR measurements.

[1] H. E. Toma, K. Araki, A. D. P. Alexiou, S. Nikolaou, S. Dovidauskas, *Coord. Chem. Rev.* **2001**, *219−221*, 225−272.
[2] H. E. Toma, C. J. Cunha, C. Cipriano, *Inorg. Chim. Acta* **1988**, *154*, 63−66.
[3] A. D. P. Alexiou, H. E. Toma, *J. Chem. Res. (S)* **1993**, 464−465.
[4] A. Spencer, G. Wilkinson, *J. Chem. Soc., Dalton Trans.* **1974**, 786−792.
[5] J. A. Baumann, D. J. Salmon, S. T. Wilson, T. J. Meyer, W. E. Hatfield, *Inorg. Chem.* **1978**, *17*, 3342−3350.
[6] M. Abe, Y. Sasaki, Y. Yamada, K. Tsukahara, S. Yano, T. Yamaguchi, M. Tominaga, I. Taniguchi, T. Ito, *Inorg. Chem.* **1996**, *35*, 6724−6734.
[7] K. Ota, H. Sasaki, T. Matsui, T. Hamaguchi, T. Yamaguchi, T. Ito, H. Kido, C. P. Kubiak, *Inorg. Chem.* **1999**, *38*, 4070−4078.
[8] I. S. Zavarine, C. P. Kubiak, T. Yamaguchi, K. Ota, T. Matsui, T. Ito, *Inorg. Chem.* **2000**, *39*, 2696−2698.
[9] J. H. Enemark, R. D. Feltham, *Coord. Chem. Rev.* **1974**, *13*, 339−406.
[10] R. Eisenberg, C. D. Meyer, *Acc. Chem. Res.* **1975**, *8*, 26−34.
[11] F. Bottomley, *Coord. Chem. Rev.* **1978**, *26*, 7−32.
[12] B. L. Westcott, J. H. Enemark *Transition Metal Nitrosyls*; John Wiley & Sons, Inc., **1999**; Vol. II: Applications and Case Studies.
[13] E. Culotta, J. D. E. Koshland, *Science* **1992**, *258*, 1862−1865.
[14] L. J. Ignarro, *Pharm. Res.* **1989**, *6*, 651−659.
[15] S. Moncada, R. M. J. Palmer, E. A. Higgs, *Pharmacol. Rev.* **1991**, *43*, 109−142.
[16] M. J. Clarke, J. B. Gaul, *Struct. Bonding (Berlin, Ger.)* **1993**, *81*, 147−181.
[17] A. R. Butler, D. L. H. Williams, *Chem. Soc. Rev.* **1993**, 233−241.
[18] M. Fontecave, J.-L. Pierre, *Bull. Soc. Chim. Fr.* **1994**, *131*, 620−631.
[19] R. J. P. Williams, *Chem. Soc. Rev.* **1996**, 77−83.
[20] D. A. Wink, J. B. Mitchell, *Free Radic. Biol. Med.* **1998**, *25*, 434−456.
[21] S. P. Fricker, *Platinum Met. Rev.* **1995**, *39*, 150−159.
[22] N. Bettache, T. Carter, J. E. T. Corrie, D. Ogden, D. R. Trentham, *Method. Enzymol.* **1996**, *268*, 266−281.
[23] S. P. Fricker, E. Slade, N. A. Powell, O. J. Vaugham, G. R. Henderson, B. A. Murrer, I. L. Megson, S. K. Bisland, F. W. Flitney, *Br. J. Pharmacol.* **1997**, *122*, 1441−1449.
[24] T. D. Carter, N. Bettache, D. Ogden, *Br. J. Pharmacol.* **1997**, *122*, 971−973.
[25] Y. Chen, R. E. Shepherd, *J. Inorg. Biochem.* **1997**, *68*, 183−193.
[26] N. A. Davies, M. T. Wilson, E. Slade, S. P. Fricker, B. A. Murrer, N. A. Powell, G. R. Henderson, *Chem. Commun.* **1997**, 47−50.
[27] P. C. Ford, J. Bourassa, K. Miranda, B. Lee, I. Lorkovic, S. Boggs, S. Kudo, L. Laverman, *Coord. Chem. Rev.* **1998**, *171*, 185−202.
[28] J. B. Godwin, T. J. Meyer, *Inorg. Chem.* **1971**, *10*, 471−474.
[29] H. Kobayashi, N. Uryû, A. Tokiwa, T. Yamaguchi, Y. Sasaki, T. Ito, *Bull. Chem. Soc. Jpn.* **1992**, *65*, 198−202.
[30] H. Kobayashi, N. Uryû, I. Mogi, R. Miyamoto, Y. Ohba, M. Iwaizumi, Y. Sasaki, A. Ohto, T. Ito, *Bull. Chem. Soc. Jpn.* **1995**, *68*, 2551−2558.
[31] M. K. Johnson, D. B. Powell, R. D. Cannon, *Spectrochim. Acta* **1981**, *37A*, 995−1006.
[32] M. K. Johnson, R. D. Cannon, D. B. Powell, *Spectrochim. Acta* **1982**, *38A*, 307−315.
[33] A. Ohto, A. Tokiwa-Yamamoto, M. Abe, T. Ito, Y. Sasaki, K. Umakoshi, R. D. Cannon, *Chem. Lett.* **1995**, 97−98.
[34] R. W. Callahan, T. J. Meyer, *Inorg. Chem.* **1977**, *16*, 574−581.
[35] M. B. Fairey, R. J. Irving, *Spectrochim. Acta* **1966**, *22*, 359−365.
[36] M. G. Gomes, C. U. Davanzo, S. C. Silva, L. G. F. Lopes, P. S. Santos, D. W. Franco, *J. Chem. Soc., Dalton Trans.* **1998**, 601−607.
[37] F. Bottomley, M. Mukaida, *J. Chem. Soc., Dalton Trans.* **1982**, 1933−1937.
[38] I. A. Bagatin, H. E. Toma, *Spectrosc. Lett.* **1996**, *29*, 1409−1416.
[39] I. A. Bagatin, H. E. Toma, *Transition Met. Chem.* **1996**, *21*, 71−76.
[40] M. Abe, Y. Sasaki, A. Nagasawa, T. Ito, *Bull. Chem. Soc. Jpn.* **1992**, *65*, 1411−1414.
[41] T. Y. Dong, H. S. Lee, T. Y. Lee, C. F. Hsieh, *J. Chin. Chem. Soc.* **1992**, *39*, 393−399.
[42] M. Abe, Y. Sasaki, Y. Yamada, K. Tsukahara, S. Yano, T. Ito, *Inorg. Chem.* **1995**, *34*, 4490−4498.
[43] M. Abe, A. Sato, T. Inomata, T. Kondo, K. Uosaki, Y. Sasaki, *J. Chem. Soc., Dalton Trans.* **2000**, 2693−2702.
[44] A. Sato, M. Abe, T. Inomata, T. Kondo, S. Ye, K. Uosaki, Y. Sasaki, *Phys. Chem. Chem. Phys.* **2001**, *3*, 3420−3426.
[45] H. E. Toma, A. D. P. Alexiou, *J. Braz. Chem. Soc.* **1995**, *6*, 267−270.
[46] H. E. Toma, A. D. P. Alexiou, *J. Chem. Res. (S)* **1995**, 134−135.
[47] A. D. P. Alexiou, H. E. Toma, *J. Chem. Res. (S)* **1997**, 338−339.

[48] H. E. Toma, A. D. P. Alexiou, S. Nikolaou, S. Dovidauskas, *Magn. Reson. Chem.* **1999**, *37*, 322−324.
[49] S. Dovidauskas, H. E. Toma, K. Araki, H. Sacco, Y. Iamamoto, *Inorg. Chim. Acta* **2000**, *305*, 206−213.
[50] S. Dovidauskas, K. Araki, H. E. Toma, *J. Porphyrins Phthalocyanines* **2000**, *4*, 727−735.
[51] K. Araki, S. Dovidauskas, H. Winnischofer, A. D. P. Alexiou, H. E. Toma, *J. Electroanal. Chem.* **2001**, *498*, 152−160.
[52] S. Nikolaou, M. Uemi, H. E. Toma, *Spectrosc. Lett.* **2001**, *34*, 267−277.
[53] J. A. Iggo, *NMR Spectroscopy in Inorganic Chemistry*; Oxford University Press Inc.: New York, **1999**.
[54] F. A. Cotton, J. G. NormanJr, *Inorg. Chim. Acta* **1972**, *6*, 411−419.
[55] E. S. Dodsworth, A. A. Vleck, A. B. P. Lever, *Inorg. Chem.* **1994**, *33*, 1045−1049.
[56] L. G. F. Lopes, M. G. Gomes, S. S. S. Borges, D. W. Franco, *Aust. J. Chem.* **1998**, *51*, 865−866.
[57] H. E. Toma, C. J. Cunha, *Can. J. Chem.* **1989**, *67*, 1632−1635.
[58] D. T. Sawyer, J. L. Roberts, *Experimental Electrochemistry for Chemists*; John Wiley & Sons, **1974**.
[59] O. Almog, A. Bino, D. Garfinkel-Shweky, *Inorg. Chim. Acta* **1993**, *213*, 99−102.
[60] G. Powell, D. T. Richens, A. Bino, *Inorg. Chim. Acta* **1995**, *232*, 167−170.
[61] T. Yamaguchi, N. Imai, T. Ito, C. P. Kubiak, *Bull. Chem. Soc. Jpn.* **2000**, *73*, 1205−1212.

Received March 11, 2002
[I02127]